Turkish Journal of Veterinary and Animal Sciences

http://journals.tubitak.gov.tr/veterinary/

Research Article

Turk J Vet Anim Sci
(2022) 46: 565-574
© TÜBİTAK
doi:10.55730/1300-0128.4227

Some anatomical studies on the kidney of goat (Capra hircus) with special reference to angioarchitecture, ultrasonography and Doppler

Amr EL KARMOTY[1,*], **Samer DAGHASH**[1], **El Shymaa ABDELNABY**[2]

[1]Department of Anatomy and Embryology, Faculty of Veterinary Medicine, Cairo University, Giza, Egypt
[2]Department of Theriogenology, Faculty of Veterinary Medicine, Cairo University, Giza, Egypt

Received: 11.01.2022 • **Accepted/Published Online:** 08.05.2022 • **Final Version:** 03.08.2022

Abstract: The present work was carried out on twenty-five goats to study the anatomy and sonar as well as Doppler vascular perfusion of kidney in the goat. The ultrasonographic scanning of goat's kidney appeared its cortex oriented as a homogenous hypoechoic area while the medullary pyramids are presented as hypoechoic-anechoic areas deeper than the cortex. The arterial supply of the kidneys of the goat was supplied by the right and the left renal arteries. The renal artery gives accessory renal artery then passing for dividing into the dorsal and the ventral renal branches. Both branches detache the caudal dorsal, caudal dorsal midzone, cranial dorsal midzone, cranial dorsal apical segmental arteries where each of segmental artery supplies the corresponding area of the kidney. The venous drainage of the goat's kidney is oriented by right and left renal veins. The renal vein receives two dorsal and ventral renal tributaries. Both renal tributaries extend to drain by cranial and caudal renal branches. The cranial renal branch extends in the mid, cranial parts of the kidney to receive the cranial apical the cranial midzone segmental veins, while the caudal renal branch passes in the mid and caudal parts of the kidney to drain by caudal and caudal midzone segmental tributaries. The RI measurements of the right cranial segmental, caudal segmental interlobar and arcuate renal arteries had the lowest coefficient of variation (CV; 5.45, 5.08, 5.79, and 3.44, respectively) with pooled SD (0.03, 0.03, 0.03, and 0.04, respectively). The RI evaluations of the left main, cranial segmental, caudal segmental, interlobar and arcuate renal arteries had the lowest CV in form of (7.31, 6.66, 5.88, 4.34, and 5.94, respectively) with SD (0.03, 0.03, 0.03, 0.02, and 0.04, respectively). The results obtained were tabulated and discussed with the available literature in different animals and analyzed by ANOVA.

Key words: Goat, anatomy, angioarchitecture, sonar, Doppler

1. Introduction

The domestic goats (Capra aegagrus hircus) are one of the oldest domesticated species, and have been used for their milk, meat, hair and skins over much of the world [**1**]. The principal function of urinary system is the maintenance of water and electrolyte homeostasis. The second major function of this system is the excretion of many toxic metabolic waste products particularly the nitrogenous compounds urea and creatinine from the body [**2**]. The morphology of kidney and their parameters of different animals especially goat was discussed by [**1**] and [**3**] as well as its ultrasonographic evaluation reported by [**4**] and [**5**]. Concerning, the angioarchitecture of blood supply of kidneys of different animals is well established by [**6–12**], as a human module. New imaging technology permits a full description of the renal anatomy, parenchyma, and blood supply [**13**]. Color and pulsed Doppler ultrasonography are considered inexpensive procedures for the diagnostic protocol in the kidney, as with Doppler modes, renal dysfunctionality diseases such as renal stenosis and acute tubular stenosis could be demonstrated by determining the changes in the renal vascular perfusion [**14, 17**]. Moreover, it has been recommended that the reduction in any artery vascular supply could be associated with the measurement of the resistance to the blood flow, which is known as resistance index (RI), as there was a negative relation between the velocity of the arterial supply and its RI [**16, 17**]. The diagnostic accuracy of the color Doppler assessment varies from study to another one [**18, 19**], this may be due to uncontrolled factors that affect the wave pattern [**20**], therefore the color-spectral Doppler may be a more accurate tool in renal functionality and dysfunctionality assessments [**17**]. In the present investigation, we assumed a goat model in order to estimate the normal reference value of the right and left main renal arteries with their branches by color and pulsed Doppler ultrasound. The objective of our study is to determine the sonographic and

* Correspondence: amr.elkarmoty@yahoo.com

Doppler evaluation of goat's kidney as a valuable domestic animal and as an animal module for human's kidney disease diagnosis and surgical approach.

2. Materials and methods

2.1. Animals

For the vasco-morphological studies of the kidneys, the study was applied on ten adult apparent healthy goats of both sexes from Giza governorate. The specimens were washed with normal saline (0.9%) through the descending aorta, then injected using formalin solution (10%) and left for 4 days before two of them were manually dissected for studying the morphology of the kidneys. For making corrosion cast method, four kidneys were injected with 60% gum milk latex colored red with Rotring ink through the descending aorta for studying the renal arterial supply and another four samples were injected with 60% gum milk latex colored blue with Rotring ink through the caudal vena cava for estimating the renal venous drainage of the goats. For ultrasonographic evaluation, five Baladi goats aging from 3 to 4 years, kept in bans with exposure to normal day light, nourished on cereal grains and green roughages, vaccinated against internal and external parasites were selected. Ten Baladi female cyclic goats were examined for 10 times daily in order to get the reference values for the renal blood vessels, animal body weight ranged from 35–55 kg. The first study is concerned with the anatomical renal blood vessels distribution, while the second study is associated with the Doppler ultrasound examination of the kidney with the vascularization pattern in the renal artery. Animals were housed in a controlled environment, at temperatures of 26 °C to 28 °C with 13 h of light and 11 h of dark/day. All goats were fasted for 10 hours prior to any Doppler observations in order to reduce any intestinal movement that could affect the color mode of the Doppler device.

2.2. Renal arteries Doppler ultrasonography

The Doppler device used is EXAGO, Echo Control Medical, France. Doppler device equipped with linear array probe 3.5–5 MHz multifrequency [**21, 22**] was used for the examination of the main renal artery and its branches. The same operator achieved all examination using the same Doppler ultrasound settings. All examinations were performed with the following settings: frequency 5–7.5 MHz, depth 3 cm, acoustic power 80%, and gain 85 dB. [**23, 24**]. The linear probe was placed after cleaning the area on the kidney of the female goat within the middle part of the known kidney in order to reach the main renal artery as shown in Figure 1, after identifying the main artery by the color mode as shown in Figure 1a, then by the another mode the gate cursor inside the artery was opened (Figure 1b) in order to obtain the spectral graph (Figure 1c). After that the cranial branch of the renal artery (Cr. Segmental RA) appeared as shown in Figures 2a–2c) and then was examined by the two Doppler modes. In addition, the caudal branch of the renal artery (Cu. Segmental RA) was examined caudally as shown in Figures 3a–3c), finally the interlobar and arcuate renal were evaluated as depicted in Figures 4a and 4b. By the spectral mode the following Doppler parameters were measured: peak systolic velocity (PSV; cm/s), end diastolic velocity (EDV; cm/s) pulsatility index (PI), resistance index (RI), and systolic /diastolic ration (S/D).

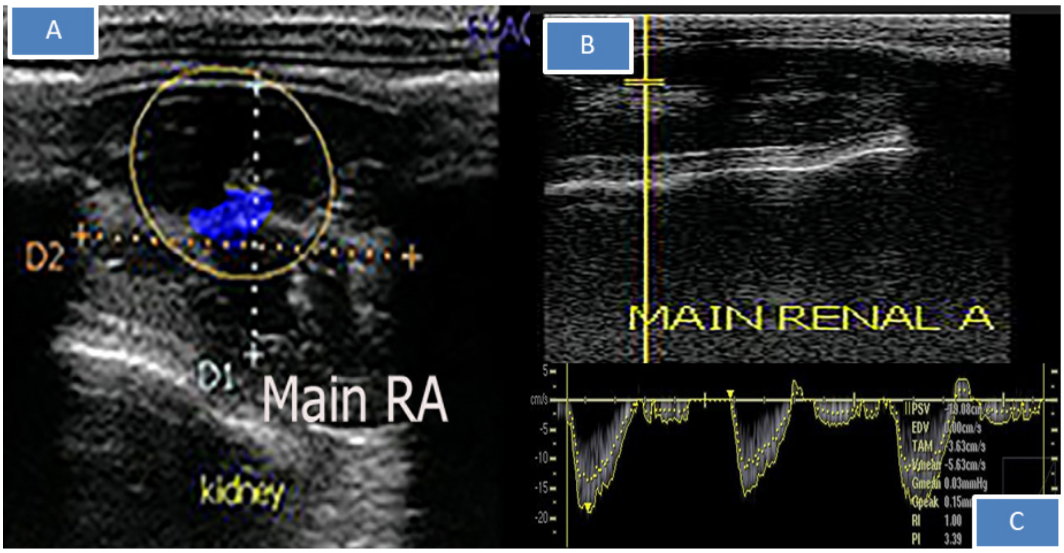

Figure 1. Typical Doppler ultrasound image of goat kidney with dimensions by B- mode and colored main renal artery (Main RA) by the color Doppler mode (A), with opening gate cursor inside the artery by the pulsed wave Doppler mode (B) in order to obtain the spectral graph (C).

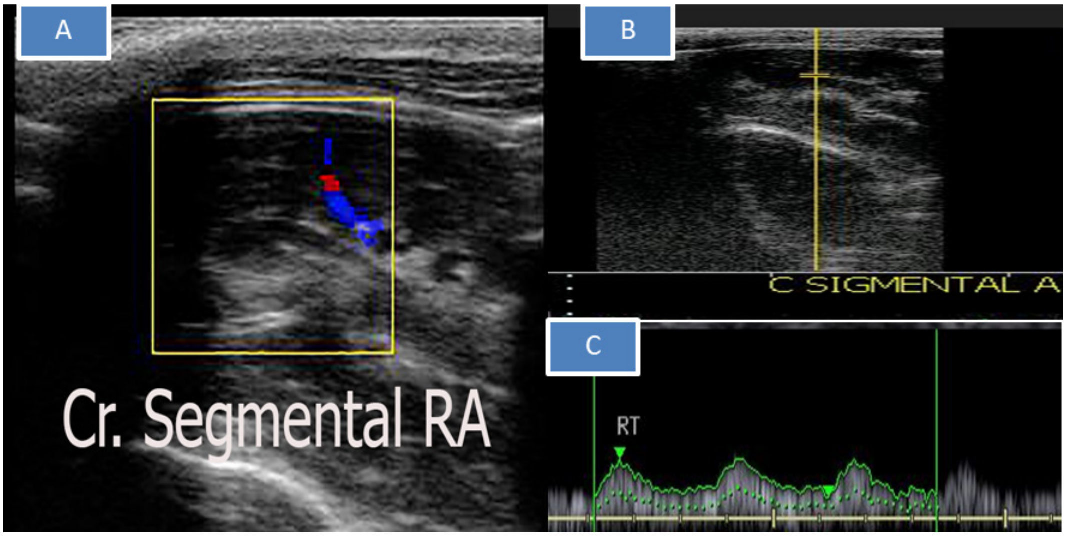

Figure 2. Typical Doppler ultrasound image of goat cranial segmental renal artery (Cr. Segmental RA) by the color Doppler mode (A), with opening gate cursor inside the artery by the pulsed wave Doppler mode (B) in order to obtain the spectral graph of systolic and diastolic ends (C).

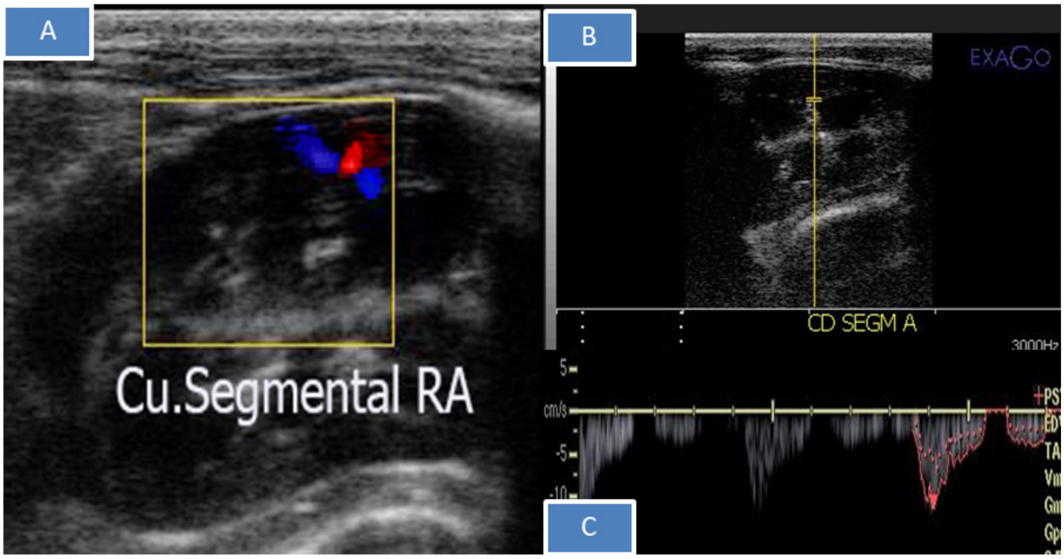

Figure 3. Typical Doppler ultrasound image of goat caudal segmental renal artery (Cu. Segmental RA) by the color Doppler mode (A), with opening gate cursor inside the artery by the pulsed wave Doppler mode (B) in order to obtain the spectral graph of systolic and diastolic ends (C).

2.3. Statistical analysis

All normal reference values of the right and left main, cranial segmental, caudal segmental, interlobar and arcuate renal arteries were measured in the form of changes in blood flow parameters. For each Doppler parameter in each branch, descriptive data analyses are obtained in the form of the mean, range, median and standard deviation (SD) across the animals and all measurements were calculated using ANOVA version 20. All data are checked for normality. One-way ANOVA was used in order to measure the variance for each Doppler velocity and each Doppler parameter. Duncan's multiple range test was used to differentiate between significant means at $p \leq 0.05$.

3. Results

3.1. Morphology of goat kidneys

The kidneys of the goat are two, smooth, bean shaped, retroperitoneal, secretory organs of the urine. They are localized asymmetrically in sublumbar region where the right kidney extends from the last rib to the 3rd lumbar

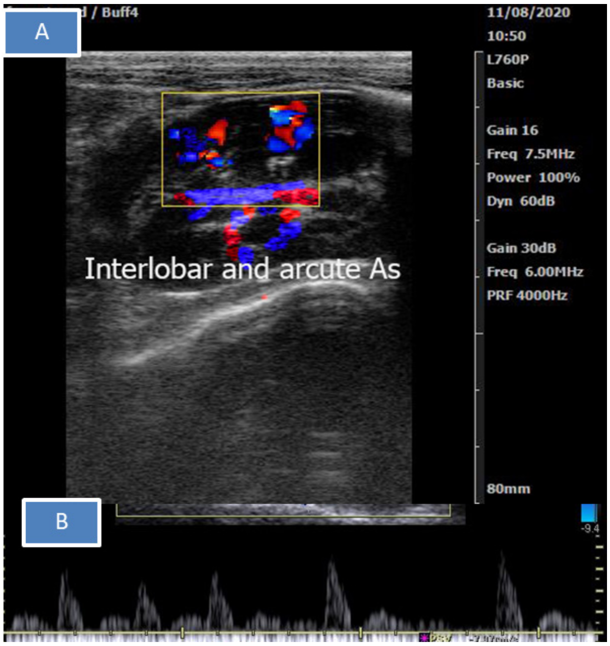

Figure 4. Typical Doppler ultrasound image of goat interlobar and arcuate renal arteries by the color Doppler mode (A) in order to obtain the spectral graph of systolic and diastolic ends (B).

transverse process (Figure 5a) while the left one extends from the caudal border of the 3rd to the 5th lumbar transverse process (Figure 5b). Externally each kidney has cranial and caudal pole, dorsal and ventral surfaces, free and attached borders where from the latter enter and leave ureter and renal vessels (Figure 5c); this depressed area is called renal hilus (Figure 5d). The former organ is measured about 55 g, 4.52 cm, 3.54 cm, and 2.92 cm in weight, length, width and thickness, respectively. The kidney of the goat is covered by thick fat capsule (Figure 5a) and thin fibrous one (Figure 5c). The former one attaches the left kidney dorsally by long mesentery (wandering kidney) and the right one adheres cranially by hepatorenal ligament. The right kidney relates dorsally to sublumbar muscles, cranially to the 1st rib, right and caudate lobes of the liver forming renal impression, pancreas and lodges medially by intestinal disc of the ascending colon. The left kidney relates dorsally to the sublumbar muscles, craniomedially to the rumen (Figure 5b) and caudally to the small intestine and the descending colon. Internally the kidney of the goat is oriented superficially by light short (1.42 cm) cortex and deeply by dark long (2.28 cm) thick medullary pyramids (Figure 5d) that separate longitudinally by thin subcortical zone (Figure 5d) from their cortical substances and transversely by collateral renal recesses for pseudo-papillae. The renal pelvis (Figure 5d) of the goat is wide, unipapillary and insinuated in the shallow renal sinus as well as it is characterized by thin renal crest and terminated by unbranched, narrow lumen ureter (Figure 5d).

3.2. Ultrasonographic evaluation

The ultrasonographic scanning was done using (ultrasound machine provided by abdominal microarray of 8.0 MHZ, Sonoscape, A5, China). The surface of goat's kidney appeared smooth and its cortex oriented as a homogenous hypoechoic area while the medullary pyramids are presented as hypoechoic-anechoic areas (Figure 6) deeper than the cortex. The renal pelvis is shown as a hypoechoic medial and deep region to the medullary areas. The randomly statistical measurements of kidney are applied on Figure 6, where the length and width are measured about 4.22 and 3.71, respectively.

3.3. Arterial renal supply

The kidneys of the goat are supplied by the right and the left renal arteries. They arise from the ventromedial wall of the abdominal aorta at the level of the midway between the 3rd and the 4th lumbar transverse process (Figures 7a and 7b). The right renal artery is longer than the left one where it measures about 5.52 cm and passes obliquely cranioventrally until it reaches its corresponding renal hilus while the left renal artery directs caudoventral oblique manner and is measured about 3.54 cm in its length. The renal artery before enters the renal hilus and gives the accessory renal artery, then passing to contribute in the vicinity of the kidney tissue where was dividing into the dorsal and the ventral renal branches. Both of dorsal (Figure 7c) and ventral branches (Figures 7c and 7d) of renal artery detache the caudal dorsal, caudal dorsal midzone, cranial dorsal midzone, cranial dorsal apical segmental arteries (Figures 7c and 7d) where each of segmental artery supplies the corresponding area of the kidney. The former arteries were terminated by arcuate arteries (Figures 7c and 7d) that give during its course in subcortical zone interlobular arteries (Figures 7c and 7d). In 20% of the examined cases, the ventral branch is represented by two separated branches (Figure 7e).

3.4. Renal venous drainage

The left and right renal veins drained into caudal vena cava. The renal vein is a large vessel, and leaves the renal hilus where it receives two dorsal and ventral renal tributaries (Figures 7f and 7g). Both dorsal (Figure 7h) and ventral renal tributaries extend in the consistency of the renal tissue to drain by cranial and caudal renal branches. The cranial renal branch (Figures 7f and 7g) extends in the mid, cranial parts of the kidney to receive the cranial apical the cranial midzone segmental veins, while the caudal renal branch (Figures 7f and 7g) passes in the mid and caudal parts of the kidney to drain by caudal and caudal midzone segmental tributaries. During examination of available specimens,

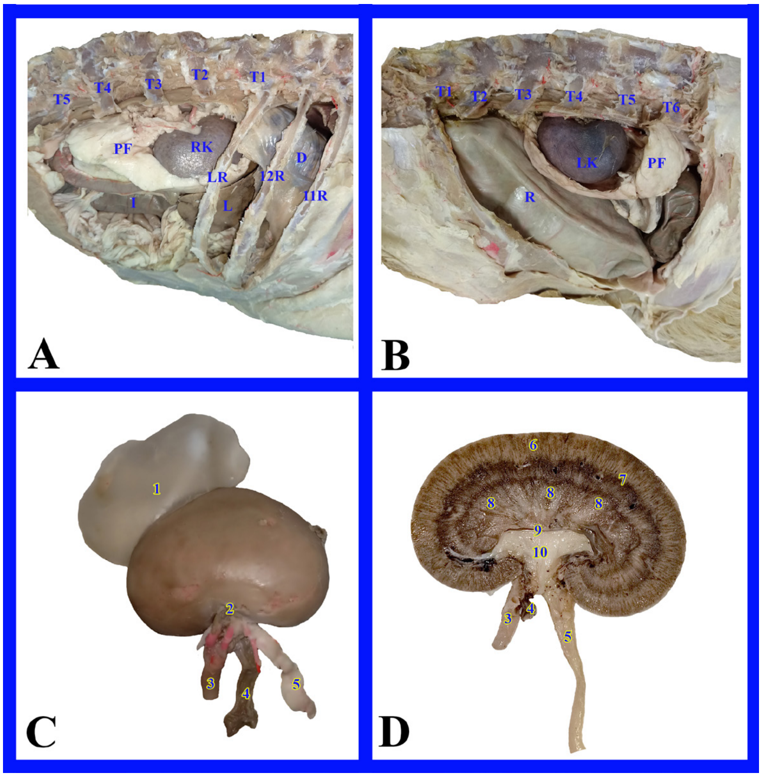

Figure 5. Morphology of kidney goat. A. Right kidney in situ. B. Left kidney in situ. C. Left kidney. D. Sagittal section left kidney. 1. Renal capsule. 2. Renal hilus. 3. Left renal A. 4. Left renal V. 5. Left ureter. 6. Renal cortex. 7. Subcortical zone. 8. Medullary pyramids. 9. Renal crest. 10. Renal pelvis. RK: Right kidney. LK: Left kidney. I: Intestine. L: Liver. D: Diaphragm. LR: Last rib. PF: Perirenal fat. T1–T6: Lumbar transverse process 1–6. 11R: 11th Rib. 12R: 12th Rib.

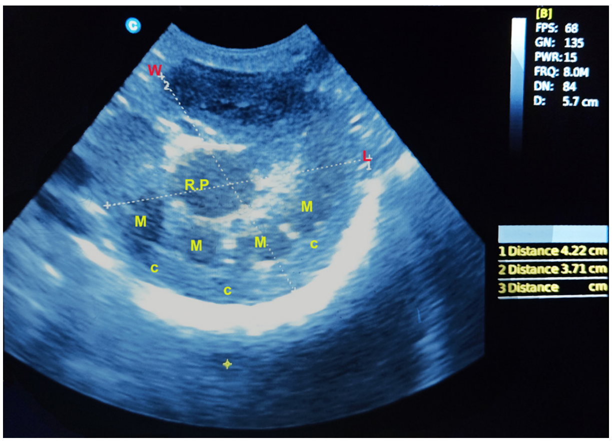

Figure 6. Ultrasonographic evaluation of the kidney goat. (C: cortex, M: medulla, RP: renal pelvis, L: length, W: width of the kidney).

30% of them (Figure 7g) had the ventral renal vein that receives cranial ventral apical segmental vein and trifurcated tributaries that includes cranial ventral midzone, caudal ventral midzone and caudal ventral segmental branches. The renal segmental veins received by arcuate venules (Figures 7f and 7g) drained during its course in subcortical zone interlobular fine tributaries (Figures 7f and 7g).

3.5. Renal vascular perfusion assessment

All Doppler parameters waveform pattern from the right and left renal artery with its branches were measured in 10 does. The data mean, range and assessments of Doppler measures calculated in both right and left renal arteries with their branches are depicted in Tables 1 and 2. The RI measurements of the right cranial segmental, caudal segmental, interlobar and arcuate renal arteries had the lowest coefficient of variation (CV; 5.45, 5.08, 5.79, and 3.44, respectively) with pooled SD (0.03, 0.03, 0.03, and 0.04, respectively) while the reference values of PI were: CV (9.77, 47.48, 42.58, and 32.12, respectively) with SD (0.13, 0.66, 0.66, and 0.54 respectively). Days of examination are significantly ($p \leq 0.05$) affected by S/D of the all right renal arteries expect the arcuate and cranial segmental renal arteries, in addition to days significantly affected by the RI of the caudal segmental renal artery ($p \leq 0.01$) as shown in Table 1 and Figure 1.

The RI evaluations of the left main, cranial segmental, caudal segmental, interlobar and arcuate renal arteries

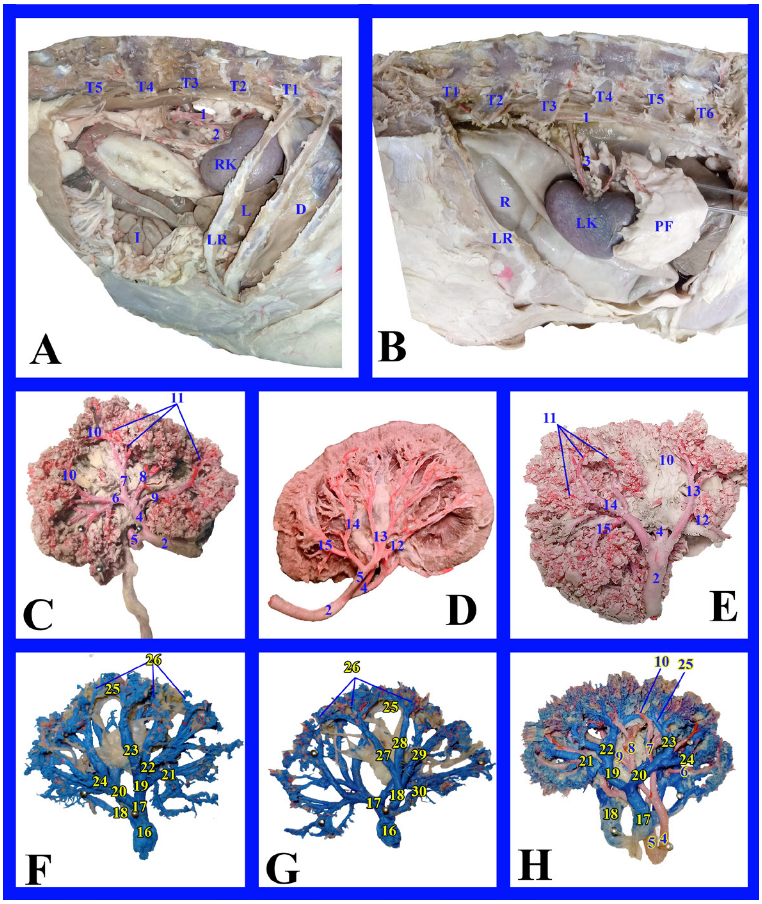

Figure 7. Angioarchitecture of goat's kidney. A. Right renal artery in situ. B. Left renal artery in situ. C. Dorsal view of left renal artery. D. Ventral view of left renal artery. E. Ventral view of left renal artery (20% exception). F. Dorsal view of right renal vein. G. Ventral view of right renal vein. H. Dorsal view of both left renal artery and vein. 1. Abdominal aorta. 2. Right renal A. 3. Left renal A. 4. Dorsal renal branch. 5. Ventral renal branch. 6. Cranial apical dorsal segmental A. 7. Cranial dorsal midzone segmental A. 8. Caudal dorsal midzone segmental A. 9. Caudal dorsal segmental A. 10. Arcuate A. 11. Interlobular A. 12. Cranial apical ventral segmental A. 13. Cranial ventral midzone segmental A. 14. Caudal ventral midzone segmental A. 15. Caudal ventral segmental A. 16. Right renal V. 17. Dorsal renal V. 18. Ventral renal V. 19. Cranial renal tributary. 20. Caudal renal tributary. 21. Cranial dorsal apical segmental V. 22. Cranial dorsal midzone segmental V. 23. Caudal dorsal midzone segmental V. 24. Caudal dorsal segmental V. 25. Arcuate V. 26. Interlobular V. 27. Cranial ventral apical segmental V. 28. Cranial ventral midzone segmental V. 29. Caudal ventral midzone segmental V. 30. Caudal ventral segmental V. RK. Right kidney. LK. Left Kidney. I. Intestine. L. Liver. D. Diaphragm. LR. Last Rib. PF. Perirenal fat. T1–T6. Lumbar transverse process 1–6.

had the lowest CV in form of (7.31, 6.66, 5.88, 4.34, and 5.94, respectively) with SD (0.03, 0.03, 0.03, 0.02, and 0.04, respectively). Days of examination are significantly ($p \leq 0.05$) affected by S/D of the all left renal arteries expect the cranial segmental and arcuate renal arteries, in addition to days significantly affected by the RI of the caudal segmental renal artery ($p \leq 0.01$) as shown in Table 2 and Figures 2–4).

4. Discussion

The kidneys of the examined goat are two, smooth, bean shaped, retroperitoneal, secretory organs of the urine. They are localized asymmetrically in sublumbar region and covered by thick fat capsule where the right kidney more cranial than the left one. These results are in agreement with that reported by **[1]** and **[3]**. We added that the right kidney extends from the last rib to the 3rd lumbar transverse process while the left one extends from the caudal border of the 3rd to the 5th lumbar transverse process. According to our finding, kidney parameters were measured about 55 g, 4.52 cm, 3.54 cm, and 2.92 cm in weight, length, width and thickness, respectively, while the results of the other study were 72 g, 6.8 cm, 4.8 cm, and 3.4 cm, respectively **[1]**. On the other hand, the results of another study were 6.2, 3.6, and 2.3 cm in length, width and thickness, respectively **[25]**. The ultrasonographic

Table 1. Summary of statistical assessments for 10 young does whose right branches were examined with sonography 10 times.

Artery	Item	Unit	Mean (Range)	SD	Normality		CV%
					p -value	Significance	
R. Main RA	PSV	cm/s	34.62 (29.14–40.11)	10.52	> 0.10	NS	30.38
	EDV	cm/s	12.96 (11.66–15.02)	8.32	> 0.10	NS	64.19
	PI		1.21 (1.19–1.23)	0.22	> 0.10	NS	18.18
	RI		0.45 (0.41–0.49)	0.11	0.06	NS	24.44
	S/D		2.67 (2.12–3.11)	0.28	0.05	*	10.48
R. Cr. Segmental RA	PSV	cm/s	31.33 (20.05–41.12)	10.31	> 0.10	NS	32.91
	EDV	cm/s	12.12 (6.11–19.36)	4.01	> 0.10	NS	33.08
	PI		1.33 (0.99–1.67)	0.13	> 0.10	NS	9.77
	RI		0.55 (0.51–0.62)	0.03	> 0.10	NS	5.45
	S/D		2.55 (2.01–2.95)	0.21	> 0.10	NS	8.22
R. Cu. Segmental RA	PSV	cm/s	29.41 (28.33–31.64)	11.32	> 0.10	NS	38.51
	EDV	cm/s	11.68 (11.21–12.36)	6.25	> 0.10	NS	53.52
	PI		1.39 (1.21–1.44)	0.66	0.07	NS	47.48
	RI		0.59 (0.49–0.68)	0.03	0.05	**	5.08
	S/D		2.51 (2.5–2.55)	0.18	0.01	*	7.17
R. Interlobar RA	PSV	cm/s	28.01 (26.96–31.01)	13.22	> 0.10	NS	47.19
	EDV	cm/s	11.43 (11.24–11.62)	2.78	0.08	NS	24.32
	PI		1.54 (1.23–1.89)	0.66	> 0.10	NS	42.85
	RI		0.69 (0.65–0.73)	0.04	0.09	NS	5.79
	S/D		2.45 (2.31–2.66)	0.31	0.01	*	12.65
R. Arcuate RA	PSV	cm/s	25.66 (23.64–27.33)	11.23	> 0.10	NS	43.77
	EDV	cm/s	9.36 (9.12–9.67)	2.08	> 0.10	NS	22.22
	PI		1.65 (1.63–1.68)	0.54	> 0.10	NS	32.12
	RI		0.87 (0.84–0.91)	0.03	> 0.10	NS	3.44
	S/D		2.75 (2.53–2.94)	0.15	> 0.10	NS	5.81

*, **, fitted to compare the significance ($p \leq 0.05, 0.01$).
R, right; RA, renal artery; Cr, cranial; Cu, caudal; PSV, peak systolic velocity; EDV, end diastolic velocity; PI, pulsatility index; RI, resistance index; S/D, systolic/diastolic.

evaluation of the surface of goat's kidney appeared smooth and its cortex oriented as a homogenous hypoechoic area while the medullary pyramids are presented as hypoechoic-anechoic areas deeper than the cortex. The renal pelvis is shown as a hypoechoic medial and deep region to the medullary areas. These statements are nearly similar to that cited by **[4, 5]**. The kidneys of the goat are supplied by the right and the left renal arteries. They arise from the ventromedial wall of the abdominal aorta. These results are in agreement with that cited by **[6, 12]**. The right renal artery is longer than the left one. The result is matched with that mentioned by **[9, 11, 8]**. On the other hand, the left renal artery is longer than the right one, these results are in agreement with that cited by **[6, 26, 12]**. The renal artery before enters the renal hilus, and gives accessory renal artery, then passing to contribute in the vicinity of the kidney tissue where was dividing into the dorsal and the ventral renal branches. These results are also reported by **[6, 9, 27, 11]**. In our study, both of dorsal and ventral branches of renal artery detache the caudal dorsal, caudal dorsal midzone, cranial dorsal midzone, cranial dorsal apical segmental arteries where each of segmental artery supplies the corresponding area of the kidney. While **[6, 9, 11, 28]** said that the dorsal and ventral branches have no cranial and caudal branches of the renal arteries, we added that in 20% of the examined cases, the ventral branch is represented by two separated branches. The segmental arteries terminated by arcuate arteries give during its

Table 2. Summary of statistical assessments for 10 young does whose left branches were examined with sonography 10 times.

Artery	Item	Unit	Mean (Range)	SD	Normality		CV%
					p –value	Significance	
L. Main RA	PSV	cm/s	32.41 (30.21–35.11)	13.54	> 0.10	NS	41.77
	EDV	cm/s	11.23 (10.66–11.39)	5.15	> 0.10	NS	45.85
	PI		1.18 (1.12–1.29)	0.21	> 0.10	NS	17.78
	RI		0.41 (0.39–0.43)	0.03	0.09	NS	7.31
	S/D		2.47 (2.25–2.66)	0.19	0.04	*	7.71
L. Cr. Segmental RA	PSV	cm/s	29.13 (25.05–31.22)	9.34	> 0.10	NS	32.06
	EDV	cm/s	11.42 (10.11–12.76)	4.51	> 0.10	NS	39.49
	PI		1.29 (1.12–1.46)	0.11	> 0.10	NS	8.55
	RI		0.45 (0.41–0.51)	0.03	> 0.10	NS	6.66
	S/D		2.41 (2.12–2.65)	0.11	> 0.10	NS	24.33
L. Cu. Segmental RA	PSV	cm/s	28.11 (27.31–29.66)	9.36	> 0.10	NS	33.29
	EDV	cm/s	9.99 (9.51–10.32)	5.22	> 0.10	NS	52.25
	PI		1.31 (1.25–1.49)	0.85	0.09	NS	64.88
	RI		0.51 (0.42–0.61)	0.03	0.04	**	5.88
	S/D		2.42 (2.22–2.64)	0.20	0.01	*	8.26
L. Interlobar RA	PSV	cm/s	27.11 (26.23–28.31)	13.22	> 0.10	NS	48.76
	EDV	cm/s	10.49 (10.01–11.11)	2.41	0.07	NS	22.97
	PI		1.54 (1.23–1.89)	0.19	> 0.10	NS	12.33
	RI		0.69 (0.65–0.73)	0.02	0.08	NS	4.34
	S/D		2.45 (2.31–2.66)	0.21	0.05	*	8.57
L. Arcuate RA	PSV	cm/s	24.16 (22.24–26.41)	10.22	> 0.10	NS	42.31
	EDV	cm/s	9.15 (9.01–9.32)	1.14	> 0.10	NS	12.49
	PI		1.61 (1.55–1.63)	0.51	> 0.10	NS	31.64
	RI		0.67 (0.63–0.71)	0.04	> 0.10	NS	5.94
	S/D		2.44 (2.21–2.53)	0.21	> 0.10	NS	8.66

*and ** fitted to compare the significance ($p \leq 0.05, 0.01$).
L, left; RA, renal artery; Cr, cranial; Cu, caudal; PSV, peak systolic velocity; EDV, end diastolic velocity; PI, pulsatility index; RI, resistance index; S/D, systolic/diastolic;
SD, standard deviation.

course in subcortical zone interlobular arteries. These statements were similar to that established by the available literatures. The renal veins of goat are right and left drained into caudal vena cava. The renal vein is a single large vessel leaving the renal hilus. The result is in agreement with that cited by [**10**] in pig**.** On the other hand in the cat [**29**]**,** dog [**30**]**,** and lion [**31**] both kidneys were drained by two renal veins. The current study revealed that the renal veins received two dorsal and ventral renal tributaries. Both dorsal and ventral renal tributaries extend in the consistency of the renal tissue to drain by cranial and caudal renal branches. These statements are in contrast to that founded by [**7, 10**] where the stem renal vein in the pig arose from three tributaries: cranial, middle and caudal renal veins. Concerning the cascade of intrarenal venous drainage distribution, the cranial renal branch extends in the mid, cranial parts of the kidney to receive the cranial apical the cranial midzone segmental veins, while the caudal renal branch passes in the mid and caudal parts of the kidney to drain by caudal and caudal midzone segmental tributaries. We added that in 30% of specimens had the ventral renal vein receives cranial ventral apical segmental vein and trifurcated tributaries that includes cranial ventral midzone, caudal ventral midzone and caudal ventral segmental branches. These results differ completely from the results discovered by [**7, 10**] where they founded that only the ventral half of the cranial and caudal thirds of the kidney were drained by the large veins represented by the cranial and caudal renal veins as well as their interlobar veins. The dorsal half was drained by small dorsal collateral veins emptied by anastomoses into the ventral set. In accordance with [**10**] in pig and [**32**] in bovine; the current renal segmental veins received by arcuate venules drained during its course in subcortical zone interlobular fine tributaries. All does showed an excessive changeability of renal Doppler measurements, as our animals were ideal for the Doppler measures with average body condition score and the renal vessels were easily detected, all examination conditions were standardized. We selected the both renal vessels in order to show any difference between them, but our result revealed that Doppler measurement of both renal arteries were the same. The Doppler velocity waveform pattern is influenced by the resistance index of the renal tissue in addition to the fluid inductance and renal vessel wall elasticity; all those factors could affect the Doppler waveform pattern [**33, 34**]. Similar to our finding, any increase in the compliance can affect the impedance by increasing without any changes in the RI and PI of the renal artery [**35, 36**]**.** Therefore, Doppler factors measurements of the renal arteries are important in the diagnosis of the renal disorders in addition to predicting the critical renal artery stenosis as previously mentioned by many authors [**37–39**]. Our study reported the increase in the renal artery blood flow PSV with the decrease in the RI, in contrast with our result, some studies showed that the increase of both PSV and RI as they concluded that both parameters are very important in detecting the severity of the renal case [**14, 38**]**.** The study finding is very relevant and important in follow-up cases if the Doppler indices as RO and PI are used, because any differences in the mentioned Doppler parameters were recorded due to any abnormal condition and could lie within the range different from the normal reference range, for examples in female goats the difference between two critical Doppler indices should be within the range (0.41–0.49) in order to be considered significant, but the PI should lie in the range (1.19–1.23) for the right branch of the renal artery, while the left one RI and PI should be within the range (0.39–0.43) and 1.12–1.29), respectively.

5. Conclusion

According to the results of our study, it can be concluded that the ultrasonographic and Doppler evaluation of the kidney of the goat is considered potential tools for predicting the whole surface anatomy and deep blood supply of the kidney that confirmed by the applied morphometrical anatomy.

Conflict of interest

The authors have no conflicts of interest to declare.

References

1. Jabbar AI, Hanaa KA, Raad SI, Alaa NL. Anatomical And Histological Investigation of the kidney in goat (Capra hircus). Diyala Journal of Agricultural Sciences 2018; 10: 1-12.
2. Chauhan RS. Text of veterinary clinical and laboratory Diagnosis, Joypee Brothers Medial Publishers (p) Ltd., New Delhi, India 1995; 110-111.
3. Al-jebori JG, Al badri AM, Jassim BA. Study the anatomical and histomorphloogical description of the kidney in adult white rabbits female ((New Zealand strain)). World Journal of Pharmaceutical science 2014; 3 (6): 40-51.
4. Ragab GA, Seif MM, Hagag UA. Radiologic and ultrasonographic studies of kidneys in goat. BS. Veterinary Medical Journal 6thScientific Conference 2010; 20 (1): 30-37.
5. Vosough D, Mozaffari AA. Evaluation of Normal Ultrasonographic Findings of Kidney in Raiini Goat. Iranian Journal of Veterinary Surgery 2009; 4: 1-2.
6. Ozdemir M, Ozüdoğru Z, Balkaya H. Arterial Vascularization of Kidneys in the Hasmer Sheep. Atatürk Üniversitesi Veteriner Bilimleri Dergisi 2018; 13 (2): 121-127, doi: 10.17094/ataunivbd.303147.
7. Farag FMM. The Intrarenal Venous Architecture of the Pig Kidney (Sus scrofa). Journal of Veterinary Anatomy 2012; 6: 1-15.
8. Paryani MR. Intrarenal patterns of the vascular supply in one humped camel (Camelus dromedarius). Annual of Biological Research 2012; 3: 4947-4950.
9. Ozdemir D, Ozudogru Z, Malkoc I. Intrarenal segmentation of the renal arteries in the Kangal dog. Journal of Faculty of Veterinary Medicine, Kafkas University 2009; 15: 41-44.
10. Filho HJ, Pereira-Sampaio MA, Favorito LA, Sam-paio FJ. Pig kidney: anatomical relationships between the intrarenal Venous Arrangement and the kidney collecting system. Journal of Urology 2008; 179: 1627-1630.
11. Aksoy G, Kurtul I, Ozcan S, Aslan K, Ozudogru Z. Intrarenal arteries and their patterns in the Tuj sheep. Journal of Veterinary Medicine 2004; 49: 57-60.
12. Ghoshal NG. Ruminant heart and arteries. In “Sisson and Grossman’s the Anatomy of the Domestic Animals”, Ed., R Getty, 5th edith 1975; 528, WB. Saunders Company, Philadelphia.
13. Maaji SM, Daniel O, Adamu B. Sonographic measurement of renal dimensions of adults in Northwestern Nigeria: a preliminary report. Sub-Saharan African Journal of veterinary Medicine 2015; 2: 123-127.

14. Granata A, Fiorini F, Andrulli S, Logias F, Gallieni M, et al. Doppler ultrasound and renal artery stenosis: An overview. J Ultrasound 2009; 12 (4): 133-143.

15. Soulez G, Oliva VL, Turpin S, Lambert R, Nicolet V et al. Imaging of renovascular hypertension: respective values of renal scintigraphy, renal Doppler US, and MR Angiography. Radiographics 2000; 20: 1355-1368.

16. Abdelnaby EA. Hemodynamic changes evaluated by Doppler ultrasonographic technology in the ovaries and uterus of dairy cattle after the puerperium. Reproductive Biology 2020; 20: 202-209.

17. Tublin ME, Bude RO, Platt JF. Review. The resistance index in renal Doppler sonography: where do we stand? American Journal of Roentgenology 2003; 180: 885-892.

18. Loubeyre P, Abidi H, Cahen R, Minh VA. Transplanted renal artery: detection of stenosis with color Doppler US. Radiology 1997; 203: 661-665.

19. Olin JW, Piedmonte MR, Young JR, Deanna S, Grubb M, et al. The utility of duplex ultrasound scanning of the renal arteries for diagnosing significant renal artery stenosis. Annual Internal Medicine 1995; 122: 833-838.

20. Keogan MT, Kliewer MA, Hertzberg BS, Delong DM, Tupler RH, et al. Renal resistance indexes: variability in Doppler US measurement in a healthy population. Radiology 1996; 199: 165–169.

21. Fouad KE, Elzomor S, Farghali H, Emam IA, Abdelnaby EA. Measurement of normal splenic blood flow indices in donkeys using color doppler ultrasound. Bioscience Research 2018; 15 (4): 4237-4242.

22. Abdelnaby EA, Abo El-Maaty AM, Ragab RSA, Seida AA. Dynamics of uterine and ovarian arteries flow velocity waveforms and their relation to follicular and luteal growth and blood flow vascularization during the estrous cycle in Friesian cows. Theriogenology 2018; 121: 112-121.

23. Abdelnaby EA, Abo El-Maaty AM. Dynamics of follicular blood flow, antrum growth, and angiogenic mediators in mares from Deviation to Ovulation. Journal of Equine Veterinary Science 2017a; 9: 51-55.

24. Abdelnaby EA, Abo El-Maaty AM. Luteal blood flow and growth in correlation to circulating angiogenic hormones after spontaneous ovulation in mares. Bulgarian Journal of Veterinary Medicine 2017b; 20: 97-109.

25. Khan H, Muhammad MR, Ahmad R , Ahmad N. Gross Anatomical Study on Normal Kidneys of Adult Goat. Journal of Animal and Veterinary Advances 2003; 2: 539-541.

26. Mazensky D, Flesarova S. Arrangement of renal arteries in guinea pig. Anatomical Record 2017; 300: 556-559.

27. Ozudogru Z, Ozdemir D. Intrarenal arterial patterns in the wolf. Veterinary Medicine 2005; 50: 411-414.

28. Aslan K, Nazli, MA. Comparative macroanatomic investigation on the intrarenal segmentation of the renal artery in goats and morkaraman sheep. Indian Veterinary Journal 2001; 78: 139-143.

29. Wesber H. Ein Beitrag Zum problem der Verdoppelung der Vena cava caudalis bie der Katze. Anatomischer Anzeiger 1968; 122: 491-495.

30. Evans HE, Christensen, GC. Miller's Anatomy of the dog. 1979. Verlag. W.B. Saunders CO. Philadelphia, London.

31. Abuzaid SM, Gad MR, Wally YR. Renal venous system of the lion (Panthera leo) a gross anatomical description. Veterinary Medical Journal. Giza Volume 1993; 41: 131-135.

32. Oliveira RR. Bovine kidney: anatomical relationships between the intrarenal Venous Arrangement and the kidney collecting system. Brazilian Journal of Morphological Science 2008; 25 (1- 4): 1-34.

33. Mostbeck GH, Gossinger HD, Mallek R, Siostrzonek P, Schneider B, et al. Effect of heart-rate on Doppler measurements of resistance index in renal-arteries. Radiology 1990; 175: 511-513.

34. Tublin ME, Tessler FN, Murphy ME. Correlation between renal vascular resistance, pulse pressure, and the resistance index in isolated perfused rabbit kidneys. Radiology 1999; 213: 258-264

35. Bude RO, Larson RG, Nichols WW, Rubin JM. Stenosis of the main artery supplying an organ: effect of end-organ vascular resistance on the poststenotic peak systolic velocity in an in vitro hydraulic model at Doppler US. Radiology 1999; 212: 79-87.

36. Bude RO, Rubin JM. Relationship between the resistance index and vascular compliance and resistance. Radiology 1999; 211: 411-417.

37. Textor SC, Wilcox CS. Renal artery stenosis: a common, treatable cause of renal failure? Annual Review of Medicine 2001; 52: 421-442.

38. Zubarev AV. Ultrasound of renal vessels. . European Radiology 2001; 11: 1902-1915.

39. Safian RD, Textor SC. Renal-artery stenosis. New England Journal of Medicine 2001; 344 (6): 431-442.